



Journal of Applied Sciences

ISSN 1812-5654

science
alert

ANSI*net*
an open access publisher
<http://ansinet.com>

RESEARCH ARTICLE

OPEN ACCESS

DOI: 10.3923/jas.2015.1210.1222

Transition Metal Complexes of (*E*)-*N'*-(4-cyanobenzylidene)nicotinohydrazide): Synthesis, Structural and Anti-Mycobacterial Activity Study

¹Kehinde O. Ogunniran, ¹Joseph A. Adekoya, ¹Cyril O. Ehi-Eromosele, ¹Tolutope O. Siyanbda, ¹Akinlolu Kayode, ¹Micheal A. Mesubi and ²Tadigoppula Narender

¹Department of Chemistry, College of Science and Technology, Covenant University, Ota, Ogun State, Nigeria

²Medicinal and Process Chemistry Division, CSIR-Central Drug Research Institute, Lucknow, India

ARTICLE INFO

Article History:

Received: June 28, 2015

Accepted: October 02, 2015

Corresponding Author:

Kehinde O. Ogunniran

Department of Chemistry,
College of Science and Technology,
Covenant University, Ota,
Ogun State, Nigeria

ABSTRACT

One step condensation of nicotinic acid hydrazide and 4-cyanobenzaldehyde formed a bidentate acylhydrazone ligand (HL⁵). The acylhydrazone was characterized by ESI mass spectrometer, CHN analyzer, IR spectrometer, ¹H-NMR, ¹³C-NMR and 2D NMR (COSY and HSQC). Thereafter, Mn(II), Mo(V), Fe(II), Cu(II) and Zn(II) complexes of the acylhydrazone ligand were synthesized and characterized based on conductivity measurements, melting point determination, CHN analysis, AAS, magnetic measurement, UV/Visible study, IR spectroscopy, ESR and TGA/DTA studies. The information obtained corroborated results from powder X-ray analysis to arrive at the model structures for the complexes. *In vitro* antimycobacterial properties of the compounds were evaluated against *Mycobacterium tuberculosis* H37Rv by using micro-diluted method. The result obtained revealed that HL⁵, Mn(II), Mo(V), Cu(II) and Zn(II) complexes exhibited promising antitubercular activity. Zn(II) complex had the highest MIC value of 0.62 µg ML⁻¹, while Fe(II) complex exhibited the lowest MIC value of 1.15 µg ML⁻¹. However, the result of cytotoxicity study indicated that acylhydrazone and Zn(II) complex with IC₅₀ of 2.17 and 1.72 µM, respectively were not toxic compared to isoniazid. Mn(II) complex was however found to be the most toxic.

Key words: Acylhydrazones, electron spin resonance, thermogravimetric, p-XRD crystallography, antitubercular agents

INTRODUCTION

Hydrazones and their derivatives are considered as versatile class of compounds in organic chemistry with interesting biological properties, such as anti-inflammatory (Thomas *et al.*, 2011), analgesic, anticonvulsant, antituberculous (Da Costa *et al.*, 2012; Gemma *et al.*, 2009), antitumor (Torje *et al.*, 2012), anti-HIV (Rollas and Kucukguzel, 2007) and antimicrobial activities (Banerjee *et al.*, 2009; Mangalam *et al.*, 2009). It has been recognized that metal complexes of the hydrazones may serve

as models for biological important species (Rakesh *et al.*, 2009). Thus, enormous interest has been shown in the field of bioinorganic chemistry toward metal complexes of the hydrazones. Hydrazones are important candidates for drug design and are potential ligands for metal complexes (Rakesh *et al.*, 2009; Gupta and Sutar, 2008). Hydrazones are widely used in organic synthesis, especially in the preparation of heterocyclic compounds due to their ability to react with electrophilic and nucleophilic reagents (Brehme *et al.*, 2007). The introduction of functional groups into hydrazones molecules through derivatization expands their unique

physical and chemical properties. Several reviews on hydrazones have shown that most of them are flexible in terms of their coordinating ability (Tripathi *et al.*, 2011; Kuriakose *et al.*, 2007; Ray *et al.*, 2008). They have a minimum of two coordinating groups, the amine and the carbonyl moieties. According to reports, the stereochemistry of the hydrazones is determined by the steric effects of the various substituents in the hydrazones moieties (Pavan *et al.*, 2010; Al-Shaalan, 2011). The coordinating sites can be increased by substituting R groups with substituents with more coordinating sites and through this, several hydrazones with better coordination ability have been synthesized (Sankar *et al.*, 2010).

Tuberculosis (*Tubercle bacillus*) is one of the world's leading causes of mortality (Da Costa *et al.*, 2012; Aboul-Fadl *et al.*, 2010). It is the only disease which does not require any vector for transmission from one person to another or across the physical boundary of countries. It is experienced by both developing and developed countries alike (Moreno *et al.*, 2010). The designation of tuberculosis as a global public health pandemic by the World Health Organization in the mid 1990s underscores the severe challenges facing the antimicrobial research community. The rise in the population of people affected by drug resistant TB (multidrug resistant/MDR-TB, extensive-drug resistant/XDR-TB) and latent TB is alarming. Though many countries do not have sufficient facilities to diagnose XDR-TB, yet in 2010 about 58 countries reported critical XDR-TB cases. Moreover, despite the alarming rate of the disease, there are limited drugs used for the treatment of XDR-TB which may also cause serious side effects. The occurrence of some three million new cases of tuberculosis per year worldwide and the emergence of new strains of *Mycobacterium tuberculosis* characterized by drug resistance or increased virulence have supported the pressing need for the evolution of newer and more potent drugs. A number of approaches such as target based drug design, combinatorial synthesis, high-throughput screening, etc. have been explored but chemical modification of a known anti-TB drug has proven a successful approach in the development of anti-TB agent (Ramon-Garcia *et al.*, 2013). It declared that TB as a global emergency but since that then, no new drug has been developed for the treatment of the disease (WHO., 2010). Moreover, due to the global emergence of multidrug-resistant tuberculosis (MDR-TB) and extensively drug resistant tuberculosis (XDR-TB) there is an urgent need to develop new anti mycobacterials (Aboul-Fadl *et al.*, 2011). Thus, it is high time a highly effective drug was discovered for the complete eradication of TB. It is in this regard that the present research work in the field of metal drugs is geared toward the synthesis and characterization of Schiff base hydrazone and some of its transition metal complexes as prospective antitubercular agents.

MATERIALS AND METHODS

Chemistry: All reagents and solvents used are of analytical grade and they were used without further purification. The metal salts used for synthesis [Mn(CH₃COO)₂, Zn(CH₃COO)₂, MoCl₅, FeCl₂, CuSO₄] were commercially obtained from Sigma. *Mycobacterial tuberculosis* H37Rv were purchased from the American Type Culture Collection.

Melting points (°C) were recorded by using Gallenkamp melting point apparatus. Sharpness of the melting point revealed the purity of the compounds (Furniss *et al.*, 1989). Elemental analyses were carried out by using Vario EL CHNS analyser at Sophisticated Analytical Instruments Facility, Central Drug Research Institute, Lucknow, India. The ESI-MS spectrum for the hydrazone was collected from Agilent 6520 Q-TOF mass spectrometer. The percentage of metal in the synthesized metal complexes was determined by using Varian spectrometer AAS-110 at Chemistry Department, Covenant University, Nigeria. The molar conductivities of the metal complexes at ambient temperature in DMF solution (10⁻³M) were measured using systronics -304 conductivity meter. The electronic data of the hydrazone and the metal complexes were obtained in methanol/DMSO by using Perkin Elmer Spectro UV-visible Double Beam UVD spectrometer between 200 and 700 nm. The infrared spectra for the hydrazone and metal complexes were recorded on Perkin-Elmer RX-1 Fourier transform infrared spectrometer using KBr pellets in the range of 4000-400 cm⁻¹. The ¹H NMR, ¹³C NMR and ²D NMR (COSY and HSQC) spectra of the hydrazone were recorded on Bruker AMX 300 FT-NMR spectrometer with DMSO-d₆ at Sophisticated Analytical Instruments Facility, Central Drug Research Institute, Lucknow, India. The magnetic susceptibility data of paramagnetic metal complexes were measured at room temperature using vibrating susceptibility magnetometer (PAR 155) with magnetic field of -10 to +10 kOe at Instrumentation center, Indian Institute of Technology, Roorkee, India. The TGA/DTA analyses of the metal complexes were carried out by heating at the rate of 10°C min⁻¹ under inert atmosphere using thermogravimetric analyser, TGA Q500 V20.8 Build 34 model at Indian Institute of Science and Technology, Hyderabad, India. The EPR spectra of the metal complexes at 77 K were recorded on a Varian E-112 spectrometer using TCNE as the standard, with 100 KHz modulation frequency, modulation amplitude 2G and 9.1 GHz microwave frequency at Sophisticated Analytical Instruments Facility, Indian Institute of Technology, Bombay, India. The X-ray powder diffraction pattern for Ni(II) complex was recorded on a Bruker AXS D8 Advance diffractometer operating in the θ : θ mode, equipped with a secondary beam graphite monochromator.

Synthesis of (E)-N'-(4-cyanobenzylidene)nicotinohydrazone: The modified version of the synthesis by Jamadar *et al.* (2012) was employed. The solution of nicotinic

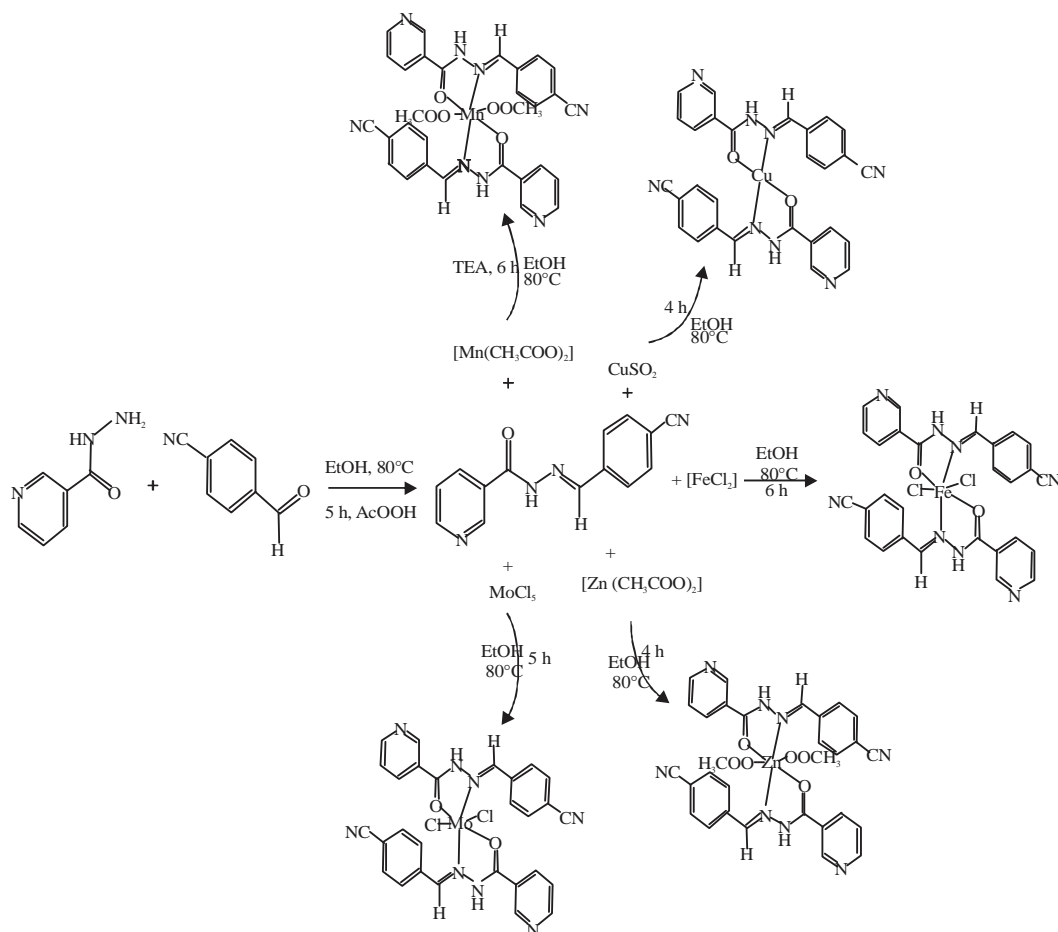


Fig. 1: Reaction path for HL⁵ and its metal complexes

acid hydrazide (10 mmole, 305 mg) in 20 mL of absolute ethanol was mixed with ethanolic solutions of 4-cyanobenzaldehydes (10 mmole, 327 mg) in 20 mL of absolute ethanol in a round bottom flask. Two drops of glacial acetic acid was added to the mixture and it was refluxed for 5 h (Fig. 1). The reaction was monitored by TLC. The precipitate obtained was filtered, washed with cold ethanol and recrystallized in a mixture of methanol and chloroform (1:1, v/v). The white crystal obtained was washed twice with another 15 mL of ethanol. The new compound was dried in vacuum and the purity confirmed by TLC (10% ethanol: 90% chloroform). Yield 1.56 g (62.4%); M.pt. 232-234°C; $R_f=0.84$ (CHCl₃/CH₃OH, 4:1, at RT); Anal.: C, 67.17; H, 4.03; N, 22.39. Found: C, 67.41; H, 3.93; N, 22.15. MS (ESI+): in m/z, Calcd. for C₁₄H₁₀N₄O [M]⁺: 250.09, Found: 251.2; ¹H NMR (300.1 MHz, DMSO-d₆) δ 12.24 (s, 1H, NH), 9.07 (s, 1H, CH), 8.77 (dd, 1H, J 4.2, H2), 8.48 (s, 1H, HCN), 8.27 (d, 1H, J 7.68, H5), 7.91 (s, 4H, H6), 7.57 (m, 1H, J 4.89, 7.68, H10), ppm. ¹³C NMR (75 MHz, DMSO-d₆) δ 161.94, 152.43, 148.62, 146.41, 138.55, 135.50, 132.72, 128.90, 127.71, 123.59, 118.5, 112.07; IR (KBr) ν/cm^{-1} : 3417, 3250 -3159, 1688, 1652, 1591, 1355, 1190, 2225.

Synthesis of Mn(HL⁵)₂(CH₃COO)₂: To a solution of HL⁵ (20 mmole, 312 mg) in ethanol, Mn(CH₃COO)₂ (10 mmole, 245 mg) dissolved in ethanol was added, followed by addition of two drops of triethylamine, while stirring at room temperature. The resulting solution was further stirred under reflux for 6 h to obtain a pale yellow product. The precipitate obtained was filtered, washed with ethanol and dried over P₄O₁₀ *in vacuo*.

Yield: 145 mg (69.05%). Elemental Anal. Found (Calcd.) (%): Mn, 8.34 (8.16); C, 56.85 (57.06); H, 4.27 (3.89); N, 17.08 (16.64). m = 5.75 BM.

Synthesis of [Mo(HL⁵)₂(Cl)₂]: Solution of HL⁵ was prepared by dissolving 20 mmole (312 mg) of the compound in 15 mL of ethanol in a double neck round bottom flask. The 10 mmole (171 mg) of MoCl₅ was weighed into an eppendorf in a fumes cupboard and transferred directly into the ethanolic solution of the HL⁵. The eppendorf was rinsed into the solution with 5 mL of absolute ethanol. The mixture was refluxed at 80°C for 5 h under nitrogen gas. The precipitate formed was filtered, washed with cold ethanol and dried over P₄O₁₀ *in vacuo*.

Yield: 0.114 g (54.54%). Elemental Anal. Found (Calcd.) (%): Mo, 14.02 (14.33); C, 50.23 (50.24); H, 3.45 (3.31); N, 16.58 (16.72), m = not determined.

Synthesis of [Fe(HL⁵)₂Cl₂]: Solution of HL⁵ (20 mmole, 312 mg, in 15 mL of methanol) prepared by heating over water bath was gradually added to equivalent of 10 mmole of FeCl₂ dissolved in 15 mL of methanol in a round bottom flask. The mixture was stirred for 30 min at ambient temperature and then refluxed at 80°C for 6 h. The black precipitate formed was filtered, washed with cold methanol, followed by ether and dried over P₄O₁₀ in vacuo.

Yield: 0.117 g (59.39%). Elemental Anal. found (Calcd.) (%): Fe, 9.04 (8.87); C, 52.52 (53.44); H, 3.61 (3.52); N, 18.09 (17.81). m = 5.2 BM.

Synthesis of [Cu(HL⁵)₂]: Ethanolic solution of HL⁵ (20 mmole, 312 mg) in a round bottom flask was warmed to 50°C on a water bath for 40 min before adding 15 mL of ethanolic solution of (10 mmole) CuSO₄. The mixture was refluxed at 80°C for 4 h. The green precipitate formed after cooling the solution in ice, it was filtered, washed with ethanol and ether and then dried over P₄O₁₀ in vacuo.

Yield: 0.124 g (68.12%). Elemental Anal. found (Calcd.) (%): Cu, 10.56 (10.92); C, 60.11 (59.84); H, 4.23 (4.50); N, 19.00 (19.25), m = 1.84 BM.

Synthesis of [Zn(HL⁵)₂(CH₃COO)₂]: A 229 mg of Zn(CH₃COO)₂ was dissolved in 20 mL of mixture of ethanol and distilled water (1:1). The solution obtained was gradually added to ethanolic solution of HL⁵ (10 mmole in 20 mL of ethanol) in a round bottom flask after which two drops of TEA was added. The solution was refluxed at 80°C for 4 h. The yellow precipitate formed was filtered, washed with ethanol and ether accordingly. The resulting compound was dried in vacuum.

Yield: 0.125 g (58.41%). Elemental Anal. found (Calcd.) (%): Zn, 9.66 (9.53); C, 55.55 (56.02); H, 4.18 (4.11); N, 16.62 (16.33), m = 0 BM.

Minimal inhibitory Concentration (MIC): The synthesized hydrazone and metal complexes were evaluated *in vitro* for anti mycobacterial activity. The compounds were screened against *M. tuberculosis* H37Rv in triplicate using broth dilution method as described by Lubert *et al.* (2003). The *M. tuberculosis* inhibitory activity of the compounds was determined through the Resazurin Microtiter Assay (REMA). Stock solutions of the test compounds were prepared in dimethyl sulfoxide (DMSO) and diluted in supplemented Middlebrook 7H9 broth (OADC enrichment-BBL/Becton Dickinson, Sparks, MD, USA), to obtain final drug concentration ranged from 0.15-250 mg mL⁻¹. The isoniazid was used as a standard drug. *Mycobacterium tuberculosis* H37Rv ATCC 35822 was grown for 7-10 days in Middlebrook

7H9 broth supplemented with OADC, plus 0.05% Tween 80 to avoid clumps. Suspensions were prepared and their turbidities matched to the optical density of the McFarland no. 1 standard. After a further dilution of 1:25 in Middlebrook 7H9 broth supplemented with OADC, 100 mL of the culture was transferred to each well of the plates together with the test compounds. Each test was set up in triplicate. Microplates were incubated for 5 days at 37°C, after which 25 mL of a freshly prepared 1:1 mixture of Alamar Blue reagent and 10% Tween 80 was added to the plate and incubated for 24 h. A blue color in the well indicated no bacterial growth and a pink color indicated growth. The Minimal Inhibition Concentration (MIC) was defined as the lowest drug concentration, which prevented a color change from blue to pink. As a standard test, the MIC of isoniazid was determined on each microplate. The acceptable range of isoniazid MIC is from 0.015-0.05 mg mL⁻¹ (Pavan *et al.*, 2010).

Cytotoxicity study: Cytotoxicity of HL⁵ and some of its synthesized metal complexes were determined with the Vero cell line ATCC CCL-81 using an MTS assay (Protopopova *et al.*, 2005).

RESULTS AND DISCUSSION

Progress has been made by Ogunniran *et al.* (2015) to synthesize (E)-N'-(4-cyanobenzylidene) nicotino-hydrazone (HL⁵) and coordinate it to selected transition metals as shown in Fig. 1. The molecular mass of HL⁵ was ascertained by the use of Agilent 6520 Q-TOF mass spectrophotometer. The mass spectrum obtained in Fig. 2, showed the molecular ion peak at (ESI) m/z 251.2 which corresponded to M+1 peak. The value obtained is in agreement with the calculated molecular mass of the compound within the precision limit of ±0.02.

¹H NMR: The ¹H NMR spectrum (Fig. 3) of the compound in DMSO-d₆ shows three singlet signals downfield of TMS at 12.24, 9.07 and 8.48 ppm. The signals were assigned to H1, H2 and H4 protons, respectively. However, a singlet signal which integrated to four hydrogen atoms appeared downfield of TMS at 7.91 ppm. The signal was attributed to the 4H6 protons in the benzonitrile ring (Adhikary *et al.*, 2014; Ogunniran *et al.*, 2015). A doublet signal at 8.77 ppm corresponds to H3 proton in the pyridyl ring. The downfield δ value is as result of de-shielding effect from adjacent N1 atom. A doublet of triplet peak at 8.28 ppm was attributed to H5 proton while the multiplet signal at 7.59 ppm was assigned to H10 proton in the pyridyl ring. The chemical shifts and multiplicity patterns are in agreement with the structure of the compound.

COSY NMR: The multiplicity and the proton assignments for HL⁵ were confirmed by COSY experiment. The COSY spectrum (Fig. 4) displayed no correlation in the benzonitrile

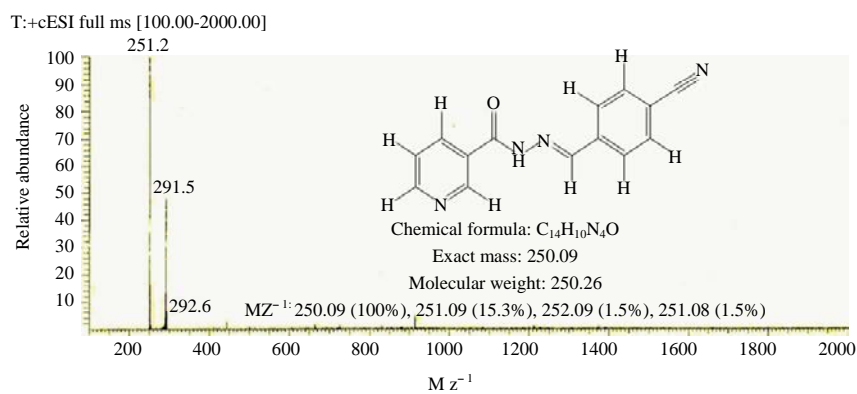


Fig. 2: ESI mass spectrum of HL⁵

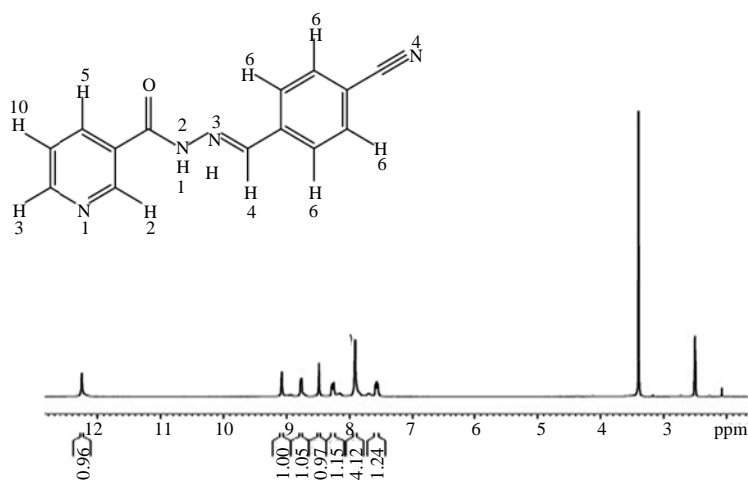


Fig. 3: ¹H NMR spectrum of HL⁵ in DMSO-d₆ at 300 MHz

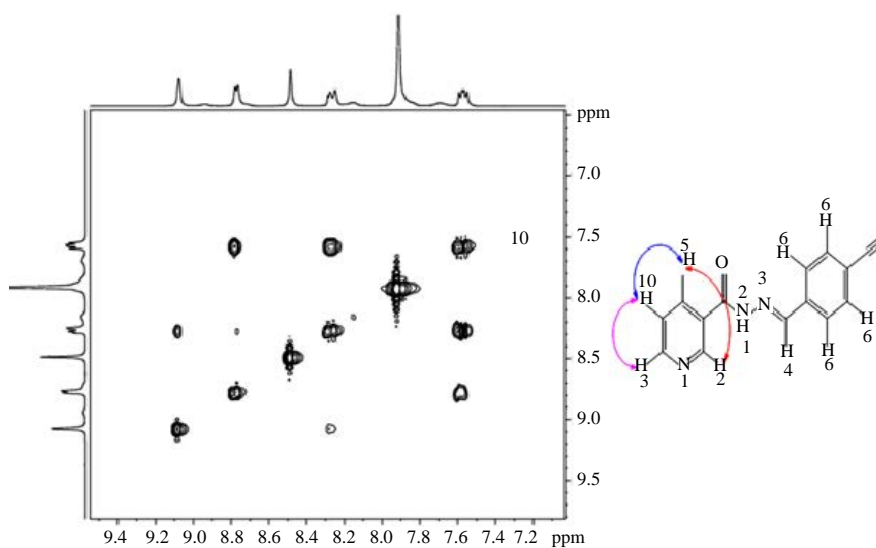


Fig. 4: ¹H-¹H COSY spectrum with schematic diagram of HL⁵ in DMSO-d₆ at 300 MHz

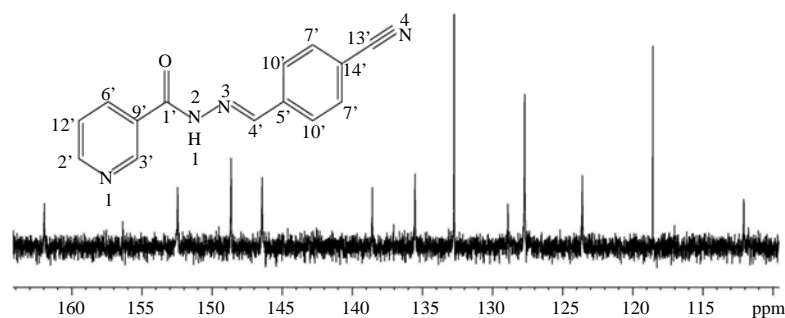


Fig. 5: ^{13}C NMR spectrum of HL^5 in DMSO-d_6 at 75 MHz

region because the four protons are in the same chemical environment and thus, resonated as a single signal at 7.91 ppm. However, off diagonal correlation was observed in the pyridyl ring region. The multiplet peak at 7.59 ppm correlated with the peaks at 8.28 and 8.77 ppm. Thus, H10 was split into multiplet while H3 and H5 were split to doublet and doublet of triplet, respectively. Meanwhile, a weak coupling effect between H5 and H3 proton was observed in the spectrum. This accounted for doublet of triplet in H5 and broad singlet in H2. Therefore, based on the observations from COSY spectrum, the ^1H - ^1H correlation schematic diagram for the hydrazone is shown in Fig. 3.

^{13}C NMR: The ^{13}C NMR spectrum for HL^5 (Fig. 5) confirmed the presence of fourteen carbon atoms in different environment in the molecule ranging from 161.94 C1-112.07 ppm, C14. The signal at 161.94 ppm was assigned to carbonyl carbon C1 based on the fact that it is the most de-shielded carbon in the molecule. The signals at 152.43 and 148.62 ppm corresponded to C2 and C3 carbons in the pyridyl ring, respectively. The two carbon atoms are adjacent to N1 atom and thus appeared downfield due to de-shielding effect from N1 atom (Ogunniran *et al.*, 2015; Ali *et al.*, 2012). The other pyridyl carbon atoms, C6, C8 and C12 were assigned to the signals at 135.50, 128.90 and 123.59 ppm, respectively. The azomethine carbon C(4) was assigned to the signal at 146.41 ppm. The signal resonated at lower field due to conjugative effect from $\text{N3} = \text{N2}-\text{C1}$ core of the molecule (Farag *et al.*, 2010). In the benzonitrile ring, C7 and C10 integrated to two carbon atoms each due to equivalent chemical environment. Hence, the signals at 132.72 and 127.71 ppm were assigned to the two carbon atoms, respectively. The signals at 138.55 and 118.57 ppm were assigned to quaternary carbons C5 and C14, respectively, while the signal at 112.07 ppm was assigned to the cyanide carbon C13.

HSQC: The ^1H - ^{13}C NMR correlation experiment was used to ascertain the ^{13}C NMR assignments. The ^1H - ^{13}C HSQC spectrum (Fig. 6) displayed seven H-C correlation as expected for HL^5 . The absence of correlation contour for carbon C1, C5,

C9, C13 and C14 confirmed these carbon atoms as non-protonated carbons. In the pyridyl ring, C2, C3, C6 and C12 showed contour correlation with hydrogen atom as assigned in both ^1H and ^{13}C NMR. The four carbon atoms in the benzonitrile ring, 2C7; 132.72 and 2C10; 127.71 ppm correlated to a signal at 7.91 ppm that integrated as four protons in the ^1H NMR. Therefore, based on HSQC spectrum, the ^1H - ^{13}C correlation schematic diagram for the hydrazone is shown in Fig. 6.

Analytical data of HL^5 and its metal complexes: The metal complexes of HL^5 are of different colour, Mn(II) complex; yellow, Mo (V) complex; green, Fe(II) complex; brown; Cu(II) complex; green and Zn(II) complex; yellow. The melting points of the complexes range from 287-304°C. All the complexes precipitated as amorphous powder. The solubility test confirmed that they were slightly soluble in methanol, chloroform, DMF and acetonitrile. However, they were soluble in DMSO and pyridine. The results of the elemental analysis are as reported in Table 1. The results show the percentage of metal content (AAS) along with the percentage of carbon, hydrogen and nitrogen present in the complexes. These are in agreement with the calculated values for the metal complexes. Thus, the results aided in deducing the formulae for the complexes. The magnetic susceptibility data recorded at ambient temperature for Mu(II), Fe(II) and Cu(II) complexes compete favorably with the calculated values. Expectedly, Zn(II) complex was found to be diamagnetic. The conductivity data obtained in DMSO confirmed the complexes as non-electrolytic nature.

Infrared spectra: The selected infrared spectra of the metal complexes were interpreted by comparing with the spectral assignments for the ligand (HL^5) (Table 2).

The multiple bands observed in the spectrum of the ligand, due to hydrogen bonding between the NH and CO group, within 3084-3417 cm^{-1} region attributed to $\nu(\text{NH})$ vibrational mode was observed as a single broad peak in the spectra of Mn(II), Fe(II), Cu(II) and Zn(II) metal complexes at lower wavelength. This is due to effect of coordination of central metal to adjacent $\nu(\text{C}-\text{O})$ group and thereby eliminates

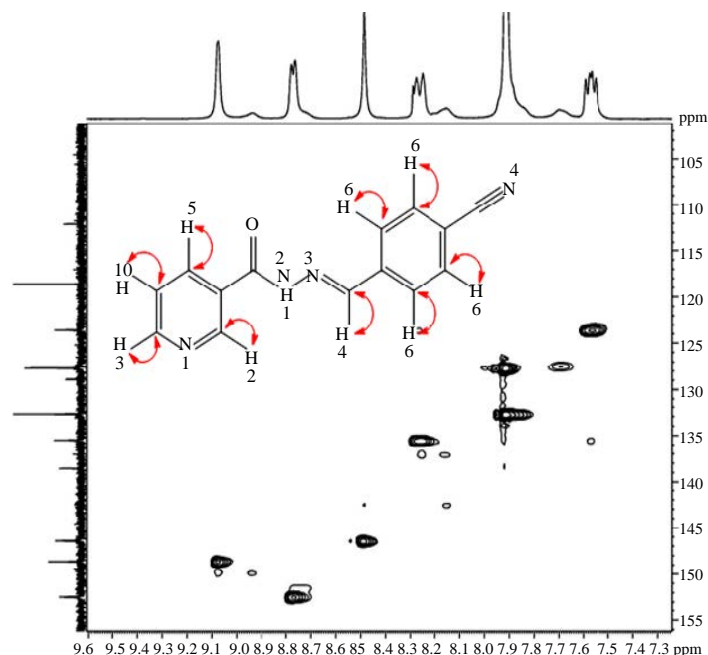


Fig. 6: ¹H-¹³C HSQC spectrum with schematic diagram of HL⁵ in DMSO-d₆ at 75 MHz

Table 1: Analytical data of HL⁵ and its metal complexes

Complex	Colour	M. pt. (°C)	Found (Calc.) %				Λ_M S cm ² mol ⁻¹	μ_{eff} μ_B
			M	C	H	N		
[Mn(HL ⁵) ₂ (CH ₃ COO) ₂] (1)	Yellow	302-304	8.34 (8.16)	56.85 (57.06)	4.27 (3.89)	17.48 (16.64)	39	5.75 (5.92)
[Mo(HL ⁵) ₂ Cl ₂] (2)	Deep brown	299-301	14.02 (14.33)	50.23 (50.24)	3.45 (3.31)	16.58 (16.74)	47	-
[Fe(HL ⁵) ₂ Cl ₂] (3)	Brown	301-302	9.04 (8.87)	52.52 (53.44)	3.61 (3.52)	18.09 (17.81)	42	5.2 (4.90)
[Cu(HL ⁵) ₂] (4)	Green	287-289	10.56 (10.92)	60.11 (59.84)	4.23 (4.50)	19.09 (19.25)	28	1.72 (1.73)
[Zn(HL ⁵) ₂ (CH ₃ COO) ₂] (5)	Light yellow	300-302	9.66 (9.53)	55.55 (56.02)	4.18 (4.11)	16.62 (16.33)	32	-

L⁵ = C₁₄H₁₀N₄O

Table 2: Infra-red data of HL⁵ and its metal complexes

Ligands/Complex	ν (NH)	ν (C = O)	ν (C = N)	δ (N-N)	δ (C-O)	δ (C-N)	ν (M-O)	ν (M-N)
	(cm ⁻¹)							
HL ⁵	3417b 3250 m,b 3159w 3084w	1688m	1652m	1591s	1355s	1190vw	-	-
[Mn(HL ⁵) ₂ (CH ₃ COO) ₂] (1)	3397s,b	1597vw	1561w	1516w	1363m	1190m	513-555w	487w
[Mo(H ₂ L ⁵) ₂ Cl ₂] (2)	3413s,b 3215vw 3164vw 3077w,b	1630vw	1600w	1528w	1392vs	1174m	591w	553m
[Fe(HL ⁵) ₂ Cl ₂] (3)	3413s,b	1669m	1596w	1409m	1355m	1153m	554w	496w
[Cu(HL ⁵) ₂] (4)	3388s,b	1618m	1517m	1454w	1380m	1143vw	515w	457m
[Zn(HL ⁵) ₂ (CH ₃ COO) ₂] (5)	3410 m,b	1602m	1518s	1472s	1368 m	1157m	527w	432 w

UV/Vis studies

existing hydrogen bond between the NH and CO in the molecule. This is further supported by tremendous reduction in the wavelength of the ν (N-N) bending vibration, which falls within the region of ν (NH) bending mode in the complexes. However, Mo(V) complexes displayed multiple bands at lower wavelength coupled with reduction in their intensities as

evidence of complexation in the molecule. This is expected for higher oxidation state metals (Davidson, 2010).

The medium band at 1688 cm⁻¹ assigned to ν (C=O) vibrational stretching in the hydrazone has undergone hypsochromic shift in the spectra of the metal complexes. The effect was attributed to coordination of the CO group to

central metal ions in the complexes. The effect of coordination through the CO group was evident by the $\nu(\text{C-O})$ deformation group which experienced a significant change in wavelength of vibration as compared to that of hydrazone. The $\nu(\text{C-O})$ deformation appeared at higher wavelength in the spectral of all the complexes except in Fe(II) complex where lower wavelength shift was observed.

A medium band at 1652 cm^{-1} attributed to azomethine, $\nu(\text{C}=\text{N})$ vibrational group in the spectrum of hydrazone has shifted to lower wavelength (16 cm^{-1}) in the metal complexes due to coordination by using a lone pair of electron on nitrogen atom and thereby reduced the intensity of vibrations. The observation was supported by negative shift observed in the bending vibration $\nu(\text{C-N})$ group in the spectra of the metal complexes as compared to hydrazone.

However, new bands, which were absent in the spectrum HL^5 , appeared at $513\text{-}591$ and $432\text{-}553\text{ cm}^{-1}$ in the metal complexes and were attributed to $\nu(\text{M-N})$ and $\nu(\text{M-O})$ vibrations, respectively. The appearance of $\nu(\text{M-N})$ and $\nu(\text{M-O})$ vibrations supports the involvement of nitrogen and oxygen atoms in complexation. The observation was attributed to effect of coordination on the group (Mobinikhaledi *et al.*, 2010).

UV/Vis studies: The electronic transition data for the ligand (HL^5) and its metal complexes in methanol are as reported in Table 3. The Mn(II) ion is of d^5 configuration with a term symbol, ^6S . As there was no sextet spin multiplicity, the d-d transitions were Laporte forbidden in this complex. However, the spectrum showed some forbidden transitions which involved the pairing of some electron spins and therefore the bands appeared very weak. The bands were observed at ca. 21142 and 18083 cm^{-1} and they were assigned to $^4\text{T}_{2g}(\text{G})$

$\leftarrow ^6\text{A}_{1g}$ and $^4\text{T}_{1g} \leftarrow ^6\text{A}_{1g}$, respectively using the Orgel diagram. The bands at ca. 49504 and 46729 cm^{-1} were assigned to $\pi \rightarrow \pi^*$ of $\text{C}=\text{N}$ and $\pi \rightarrow \pi^*$ of $\text{C}=\text{C}$, respectively, while the bands at ca. 32573 cm^{-1} could be as a result of $n \rightarrow \pi^*$ transition for both $\text{C}=\text{N}$ and $\text{C}=\text{O}$ chromophoric groups because of the broadness and the high intensity of the bands. Notwithstanding, they were thought to have undergone a hypsochromic shift, due to the effect of complexation (Chandra and Ruchi, 2013). The magnetic moment of 5.75 BM recorded for the complex strongly supported octahedral geometry for the complex.

Mo(V) spectrum showed intra-ligand transitions, with lower wave numbers shift at ca. 49504 and 47619 cm^{-1} which were attributed to $\pi \rightarrow \pi^*$ of $\text{C}\equiv\text{N}$ and $\text{C}=\text{C}$, respectively. The band at ca. 32573 cm^{-1} was assigned to transitions due to $n \rightarrow \pi^*$ of $\text{C}=\text{N}$ and $\text{C}=\text{O}$ groups. Since, Mo (V) is of high spin d^5 configuration, no d-d transition is expected. However, the spectrum showed a weak band at ca. 15432 cm^{-1} , which was attributed to the forbidden transitions in the complex and was assigned to $^5\text{T}_{2g}(\text{G}) \leftarrow ^7\text{A}_{1g}$ transition which is the characteristic of octahedral geometry (Kozakov *et al.*, 2011).

Fe(II) ion is of d^6 configuration with a term symbol, ^5D in an octahedral geometry, therefore only one absorption is expected around 15000 cm^{-1} . The spectrum of the complex shows two significant absorption bands in visible region at ca. 20576 and 16077 cm^{-1} . The first band was assigned to Metal-Ligand Charge Transfer (MLCT) while the second band was assigned to $^5\text{E}_g(\text{D}) \leftarrow ^5\text{T}_{2g}$ transition. The spectrum also shows intra-ligand bands at ca. 49504 , 45045 and 32573 cm^{-1} . Also, the magnetic moment of 5.2 BM obtained for the complex supported the assigned octahedral geometry. Deviation from the calculated spin only magnetic moment was attributed to orbital contribution (Adhikary *et al.*, 2014).

Table 3: Electronic data of HL^5 and its metal complexes

Compounds	Transition (cm^{-1})	Ground term symbol	Transition
HL^5	49019 45454 32362	-	$\pi \rightarrow \pi^*$ ($\text{C} \equiv \text{N}$) ar $\pi \rightarrow \pi^*$ ($\text{C}=\text{C}$) $n \rightarrow \pi^*$ ($\text{C}=\text{N}$, $\text{C}=\text{O}$)
$[\text{Mn}(\text{HL}^5)(\text{CH}_3\text{COO})_2]$ (1)	49504 46729 32573 21142 18083	^6S	$\pi \rightarrow \pi^*$ ($\text{C} \equiv \text{N}$) $\pi \rightarrow \pi^*$ ($\text{C}=\text{C}$) $\pi \rightarrow \pi^*$ ($\text{C}=\text{C}$) $n \rightarrow \pi^*$ ($\text{C}=\text{N}$, $\text{C}=\text{O}$) $^4\text{T}_{2g}(\text{G}) \leftarrow ^6\text{A}_{1g}$ $^4\text{T}_{1g} \leftarrow ^6\text{A}_{1g}$
$[\text{Mo}(\text{HL}^5)_2\text{Cl}_2]$ (2)	49504 47619(sh) 32573 15432	^5D	$\pi \rightarrow \pi^*$ ($\text{C} \equiv \text{N}$) $\pi \rightarrow \pi^*$ ($\text{C}=\text{C}$) $n \rightarrow \pi^*$ ($\text{C}=\text{N}$, $\text{C}=\text{O}$) $^5\text{T}_{2g}(\text{G}) \leftarrow ^7\text{A}_{1g}$
$[\text{Fe}(\text{HL}^5)_2\text{Cl}_2]$ (3)	49504 45045 32573 20576 16077	^5D	$\pi \rightarrow \pi^*$ ($\text{C} \equiv \text{N}$) $\pi \rightarrow \pi^*$ ($\text{C}=\text{C}$) $n \rightarrow \pi^*$ ($\text{C}=\text{N}$, $\text{C}=\text{O}$) MLCT $^5\text{E}_g(\text{D}) \leftarrow ^5\text{T}_{2g}$
$\text{Cu}(\text{HL}^5)_2$ (4)	44643 38314	^2S	$\pi \rightarrow \pi^*$ ($\text{C}=\text{C}$) $n \rightarrow \pi^*$ ($\text{C}=\text{N}$, $\text{C}=\text{O}$)
$[\text{Zn}(\text{HL}^5)_2(\text{CH}_3\text{COO})_2]$ (5)	45454 34602 33554 29325 13981	^1S	$\pi \rightarrow \pi^*$ ($\text{C}=\text{C}$) $n \rightarrow \pi^*$ ($\text{C}=\text{N}$, $\text{C}=\text{O}$) MLCT MLCT MLCT

Table 4: p-Xray diffraction data for [Fe(HL⁵)₂Cl₂]

Peaks	2θ°	d _{obs} (Å)	Intensity count	Intensity (%)	1/d ²	(1/d ²)/Z	h k l
1	8.076	10.9384	212	100.0	0.00836	1	0 1 0
2	9.393	9.40761	118	55.6	0.0113	1	1 0 0
3	13.865	6.38205	99.2	46.9	0.02455	2	1 1 0
4	15.877	5.57733	105	49.8	0.03115	3	1 1 1
5	16.8	5.27297	121	57.1	0.03597	3	1 1 1
6	19.79	4.48265	85	40.2	0.04977	5	2 1 0
7	23.098	3.84749	115	54.5	0.06755	6	2 1 1
8	25.738	3.45851	122	57.8	0.0836	7	2 0 2
9	32.067	2.78889	83.1	39.3	0.1285	1	3 0 0
10	48.277	1.88364	62.5	29.5	0.2818	2	3 1 0
11	67.299	1.39015	50.8	24.0	0.5175	4	3 2 0
12	83.737	1.15414	44.6	21.1	0.7507	6	3 2 1

The spectrum of Cu(II) complex did not show any band in the visible region. The two bands observed at ca. 44643 and 38314 cm⁻¹ were considered to be intra-ligand transitions. The band at 49019 cm⁻¹ in the spectrum of the ligand could not be found in the complex probably due to distortion effects. The magnetic susceptibility for the complex was found to be 1.72 BM. The value is within the range of 1.7-2.2 BM which is usually observed for Cu(II) complexes regardless of geometry. Thus, the complex was proposed to be of tetrahedral geometry.

In Zn(II) complex, no d-d transition is expected due to the fact that Zn(II) ion has a d¹⁰ configuration. However, the spectrum of the complex shows some bands at ca. 33554, 29325 and 13981 cm⁻¹ which were assigned to metal-ligand charge transfers. The bands at ca. 45454 and 34602 cm⁻¹ were assigned to π→π* (C = C) and n→π* (C = N, C = O), respectively but the π→π* (C≡N) could not be found in the spectrum due to the complexation of the ligand to Zn(II) which might have shifted the frequency of the expected band lower than 10000 cm⁻¹. The structure was proposed to be of octahedral geometry.

TGA/DTA analysis: The TGA/DTA analysis was carried out for Mo(V) complex in inert atmosphere and recorded at the rate of 10°C min⁻¹ from ambient temperature up to 700°C is shown in Fig. 7. The curve shows that the complex was stable to heat up to 180°C. However, the compound decomposed in one step within the temperature range of 200-425°C. The decomposition correlated with 73% (Cald. 74%) weight loss in the complex. The residue, which is assumed to be metallic chloride was found experimentally to be 26% of the complex. The thermogram revealed absence of coordinated water in the complex.

ESR studies: The ESR spectra study was done for Cu(II) and Mo(V) complexes. They were recorded in DMSO at liquid nitrogen temperature as shown in Fig. 8. The EPR spectrum of the Cu(II) complex gave three g values with g_{iso} = 2.1369, g_⊥ = 2.1760 and g = 1.7532. The spectrum did show three weak hyperfine splitting at 240- 255 mT due to high relaxation

time. However, since g_⊥ > g, a square planar geometry was proposed for the complex (Tachibana *et al.*, 1987). The weak hyperfine splitting observed in the spectrum at 300 mT raised the possibility of distorted tetrahedral geometry.

The X-band EPR spectrum of Mo(V) complex is characterized by only one single line with unresolved parallel and perpendicular components. The EPR parameter were found to be g_⊥ = 1.9454, g = 2.0518 and g_{av} = 1.9454. The g_{av} value supports the fact that the complex is a monomeric complex. However, since g_⊥ > g, an octahedral geometry was proposed for the complex (Huang and Jun, 1969).

p-XRD study: The crystal lattice parameters for Fe(II) complex was measured by using a Bruker AXS D8 Advance diffractometer employing Cu-Kα radiation in the range 5° to 120°, 2θ value. The powder X-ray diffraction pattern of the complex with respect to major peaks of relative intensity greater than 10% (Fig. 9) was indexed (Lipson and Taylor, 1949; Furniss *et al.*, 1989; Jamadar *et al.*, 2012). The indexing method yields the Miller indices (hkl) (Table 4), the unit cell parameters and the unit cell volume. The unit cell for Fe(II) complex yielded values of lattice constants: a = 18.357 Å, b = 21.540 Å and c = 14.976 Å and a unit cell volume V = 5921.656 Å³. The parameters corresponded with orthorhombic lattice system in which the conditions such as a ≠ b ≠ c and α = β = γ = 90° were satisfied.

On the basis of analytical data and spectroscopic data obtained, the proposed structures of Mn(II), Zn(II), Mo(V), Fe(II) and Cu(II) the complexes are shown in Fig. 10.

Antimycobacterial study: The *in vitro* anti-*M. tuberculosis* properties of the synthesized hydrazone (HL5) and the metal complexes were evaluated against *M. tuberculosis* H37Rv ATCC 35822 and the results for the Minimum Inhibitory Concentrations (MICs) are reported in Table 5. The compounds displayed MIC of 0.62 μg mL⁻¹ (ZnL⁵), 0.76 μg mL⁻¹ (MoL⁵), 0.76 μg mL⁻¹ (CuL⁵), 0.77 μg mL⁻¹ (MnL⁵), 1.15 μg mL⁻¹ (FeL⁵) and 087 μg mL⁻¹ (HL⁵) which were comparable to or better than the MIC of some “Second-line” drugs such as streptomycin

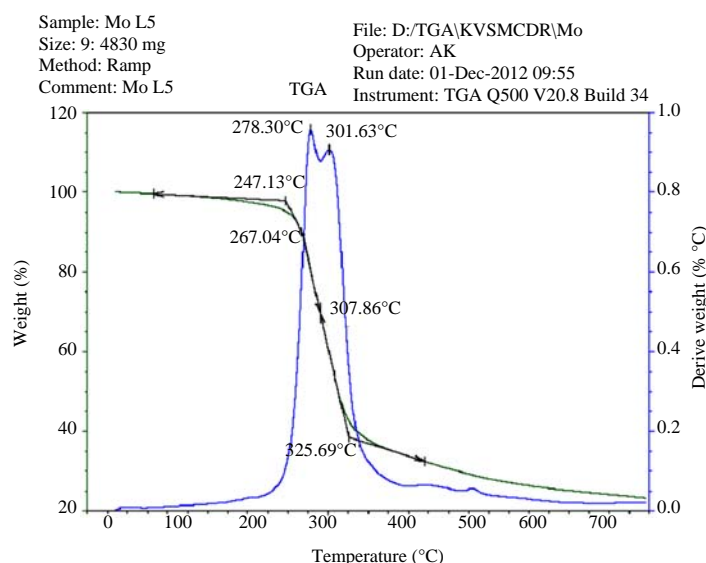


Fig. 7: DTA/TGA spectrum for $[Mo(HL^5)_2Cl_2]$

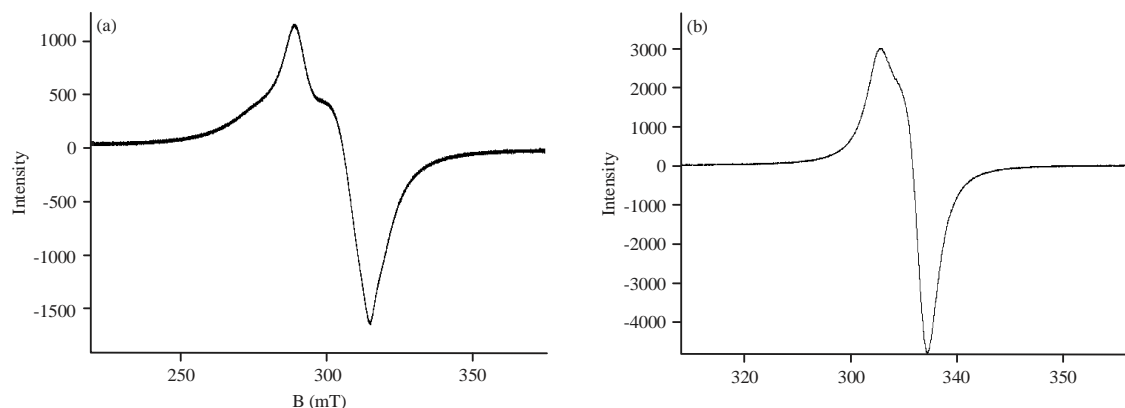


Fig. 8(a-b): EPR spectrum (a) $[Cu(HL^5)_2]$ and (b) $[Mo(HL^5)_2Cl_2]$, respectively in DMSO at 77 K

(MIC = 1.00 $\mu\text{g mL}^{-1}$), ciprofloxacin (MIC = 2.00 $\mu\text{g mL}^{-1}$), p-aminosalicylic acid (MIC = 0.5-2.0 $\mu\text{g mL}^{-1}$), ethionamide (MIC = 0.63-1.25 $\mu\text{g mL}^{-1}$), cycloserine (MIC = 12.5-50 $\mu\text{g mL}^{-1}$), gentamicin (MIC = 2.0-4.0 $\mu\text{g mL}^{-1}$), ethambutol (MIC = 0.94-1.88 $\mu\text{g mL}^{-1}$), kanamycin (MIC = 1.25-5.0 $\mu\text{g mL}^{-1}$), tobramycin (MIC = 4.0-8.0 $\mu\text{g mL}^{-1}$), clarithromycin (MIC = 8.0-16 $\mu\text{g mL}^{-1}$) and thiacetazone (MIC = 0.125-2.0 $\mu\text{g mL}^{-1}$) (Collins and Franzblau, 1997). The data (Table 5) were reproducible with minimal variation for 4 separate experiments but varied significantly from previously published MIC values and this could be attributed to the differences in protocols for MIC determination. The compounds demonstrated significant activity against *M. tuberculosis*. The test of significance also revealed that the MIC values for the complexes, except FeL^5 complex were significantly different from the isoniazid

Table 5: Minimal inhibition concentration and IC_{50} values of the metal complexes of HL^5

Compound code	MIC ($\mu\text{g mL}^{-1}$)	IC_{50} (μM)
MnL^5 (1)	0.77±0.027	0.91
MoL^5 (2)	0.76±0.031	1.02
FeL^5 (3)	1.15±0.027	0.93
CuL^5 (4)	0.76±0.033	1.13
ZnL^5 (5)	0.62±0.102	1.72
HL^5	0.87±0.34	2.17
INH (Control) = 0.91±0.133 ($\mu\text{g mL}^{-1}$)		

value (0.91 $\mu\text{g mL}^{-1}$). These results revealed that HL^5 , ZnL^5 , MnL^5 , MoL^5 and CuL^5 are potential anti-tubercular agents. The compounds were then assessed for cytotoxicity using an *in vitro* assay with monkey kidney Vero cells (Table 5). The *in vitro* cytotoxicity results for the ligand and the metal complexes assayed with monkey kidney vero cells are presented in Table 5 and Fig. 11. The result obtained

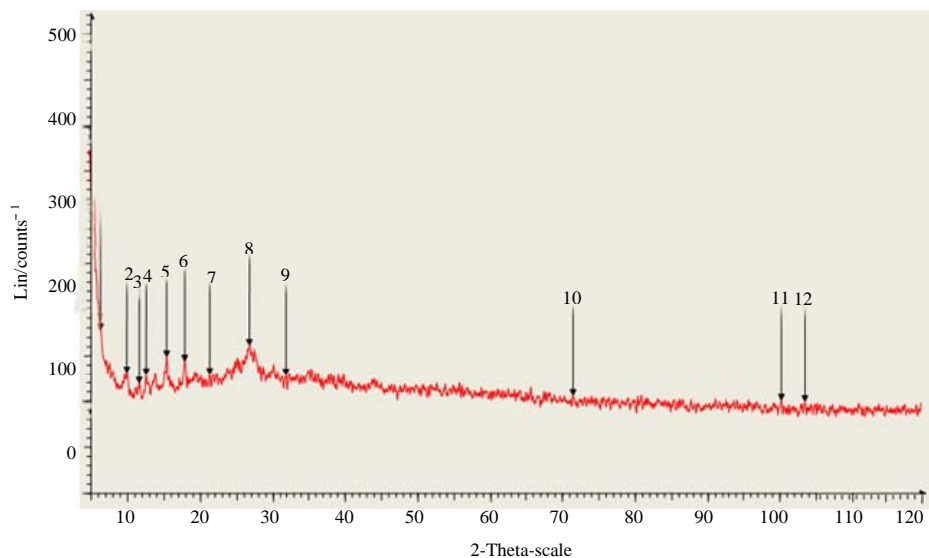


Fig. 9: p-Xray diffraction pattern of [Fe(HL⁵)₂Cl₂]

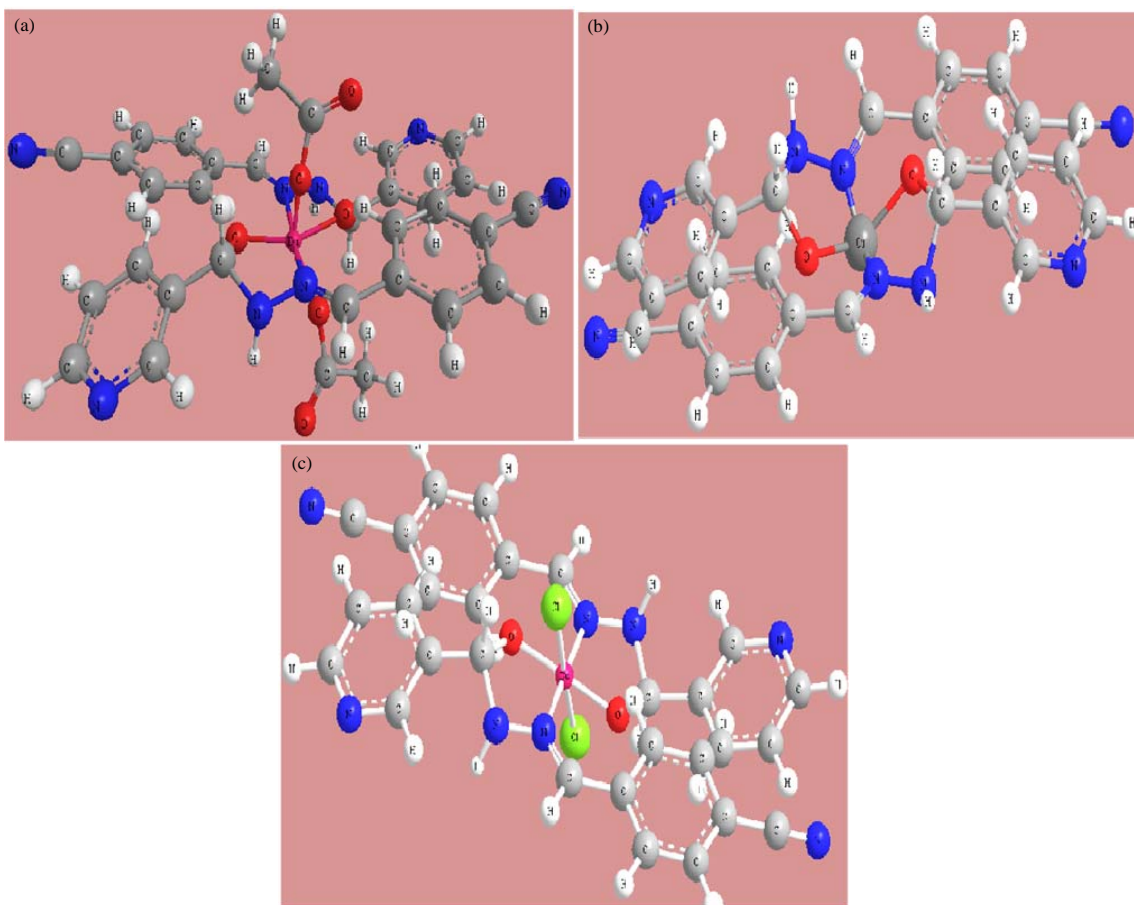


Fig. 10(a-c): Comparing of MIC ($\mu\text{g mL}^{-1}$) values of the metal complexes with the ligand and isoniazid drug, (a) Du = Mn for [Mn (HL⁵)₂ (CH₃) COO]₂], Zn for (HL⁵)₂ (CH₃COO)₂], (b) [Cu (HL⁵)₂] and (c) Du = Mn for [Mn (HL⁵)₂ (CL₂)] Fe for [Fe (HL⁵)₂ (Cl)₂]

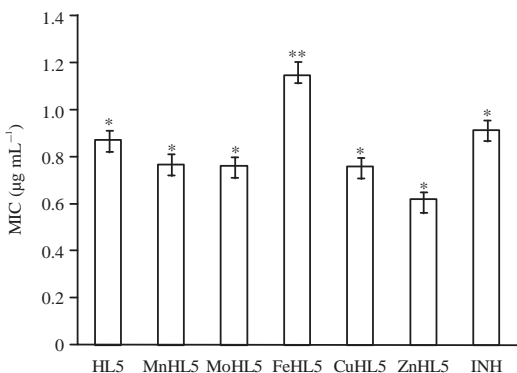


Fig. 11: Proposed schematic structures of the metal complexes

indicates that HL⁵ recorded the least toxicity while MnL⁵ was found to be the most toxic compound. The ligand displayed moderate toxicity compared to the isoniazid.

CONCLUSION

In conclusion, a novel (E)-N'-(4-cyanobenzylidene) nicotinohydrazone was successfully synthesized from nicotinic hydrazide by simple condensation reaction. The hydrazone was fully characterized by one and two dimensional NMR techniques and X-ray crystallographic study. Efforts to grow single crystals of the metal complexes did not yield positive result. Hence, the structures of the metal complexes were elucidated based on analytical data, ESR, magnetic measurement, DTA/TGA and powder X-ray analysis. The anti-tubercular potential of the compounds are established. The hydrazone and four of the metal complexes showed improved anti-tubercular potency than some of the standard drugs.

ACKNOWLEDGMENTS

The study was supported by CISR and TWAS through TWAS-CSIR fellowship. The authors are thankful as well to the technical staff of the Sophisticated Analytical Instrument Facility at Central Drug Research Institute, Lucknow, Indian Institute of Technology, Roorkee and the Indian Institute of Technology, Bombay, India for technical support.

REFERENCES

Aboul-Fadl, T., F.A.S. Bin-Jubair and O. Aboul-Wafa, 2010. Schiff bases of indoline-2,3-dione (isatin) derivatives and nalidixic acid carbohydrazide, synthesis, antitubercular activity and pharmacophoric model building. *Eur. J. Med. Chem.*, 45: 4578-4586.

Aboul-Fadl, T., H.A. Abdel-Aziz, M.K. Abdel-Hamid, T. Elsaman, J. Thanassi and M.J. Pucci, 2011. Schiff bases of indoline-2,3-dione: Potential novel inhibitors of mycobacterium tuberculosis (Mtb) DNA gyrase. *Molecules*, 16: 7864-7879.

Adhikary, A., J.A. Sheikh, A.D. Konar and S. Konar, 2014. Synthesis, crystal structure, magnetic study and magneto-structural correlation of three Cu(II) complexes formed via pyridine bis(hydrazone) based ligand. *RSC Adv.*, 4: 12408-12414.

Al-Shaalan, N.H., 2011. Synthesis, characterization and biological activities of Cu(II), Co(II), Mn(II), Fe(II) and UO₂(VI) complexes with a new Schiff base hydrazone: *O*-Hydroxyacetophenone-7-chloro-4-quinoline hydrazone. *Molecules*, 16: 8629-8645.

Ali, K.A., M.A. Elsayed and A.M. Farag, 2012. Synthesis of some new pyridine-2,6-bis-heterocycles. *HeteroCycles*, 85: 1913-1923.

Banerjee, S., S. Mondal, W. Chakraborty, S. Sen and R. Gachhui *et al.*, 2009. Syntheses, X-ray crystal structures, DNA binding, oxidative cleavage activities and antimicrobial studies of two Cu(II) hydrazone complexes. *Polyhedron*, 28: 2785-2791.

Brehme, R., D. Enders, R. Fernandez and J.M. Lassaletta, 2007. Aldehyde *N,N*-dialkylhydrazones as neutral acyl anion equivalents: Umpolung of the imine reactivity. *Eur. J. Org. Chem.*, 34: 5629-5660.

Chandra, S. and Ruchi, 2013. Synthesis, spectroscopic characterization, molecular modeling and antimicrobial activities of Mn(II), Co(II), Ni(II), Cu(II) complexes containing the tetradentate aza Schiff base ligand. *Spectrochimica Acta Part A: Mol. Biomol. Spectrosc.*, 103: 338-348.

Collins, L. and S.G. Franzblau, 1997. Microplate alamar blue assay versus BACTEC 460 system for high-throughput screening of compounds against *Mycobacterium tuberculosis* and *Mycobacterium avium*. *Antimicrob. Agents Chemother.*, 41: 1004-1009.

Da Costa, C.F., A.C. Pinheiro, M.V. de Almeida, M.C.S. Lourenco and M.V.N. de Souza, 2012. Synthesis and antitubercular activity of novel amino acid derivatives. *Chem. Biol. Drug Des.*, 79: 216-222.

Davidson, G., 2010. Spectroscopic Properties of Inorganic and Organometallic Compounds. Royal Society of Chemistry, London, UK., pp: 226-330.

Farag, A.M., K.A.K. Ali, T.M.A. El-Debss, A.S. Mayhoub, A.G.E. Amr, N.A. Abdel-Hafez and M.M. Abdulla, 2010. Design, synthesis and structure-activity relationship study of novel pyrazole-based heterocycles as potential antitumor agents. *Eur. J. Med. Chem.*, 45: 5887-5898.

Furniss, B.S., A.J. Hannaford, P.W.G. Smith and A.R. Tatchell, 1989. Vogel's Textbook of Practical Organic Chemistry. 5th Edn., Harlow, Longman, ISBN: 0-582-46236-3.

Gemma, S., L. Savini, M. Altarelli, P. Tripaldi and L. Chiasserini *et al.*, 2009. Development of antitubercular compounds based on a 4-quinolyhydrazone scaffold. Further structure-activity relationship studies. *Bioorg. Med. Chem.*, 17: 6063-6072.

- Gupta, K.C. and A.K. Sutar, 2008. Catalytic activities of Schiff base transition metal complexes. *Coordinat. Chem. Rev.*, 252: 1420-1450.
- Huang, T.J. and G.P.H. Jun, 1969. Electron spin resonance studies of monomer-dimer equilibria involving molybdenum(V) complexes with cysteine and glutathione. *J. Chem. Soc. D.*, 17: 985-986.
- Jamadar, A., A.K. Duhme-Klair, K. Vemuri, M. Sritharan, P. Dandawate and Padhye, 2012. Synthesis, characterisation and antitubercular activities of a series of pyruvate-containing aroylhydrazones and their Cu-complexes. *Dalton Trans.*, 41: 9192-9201.
- Kozakov, A.T., A.G. Kochur, A.V. Nikolsky, A.K. Googlev, A.G. Smotrakov and V.V. Eremkin, 2011. Valence and magnetic state of transition-metal and rare-earth ions in single-crystal multiferroics RMn_2O_5 (R = Y, Bi, Eu, Gd) from X-ray photoelectron spectroscopy data. *J. Electron Spectrosc. Relat. Phenom.*, 184: 508-516.
- Kuriakose, M., M.R.P. Kurup and E. Suresh, 2007. Spectral characterization and crystal structure of 2-benzoylpyridine nicotinoyl hydrazone. *Spectrochimica Acta Part A: Mol. Biomol. Spectrosc.*, 66: 353-358.
- Lipson, H. and C.A. Taylor, 1949. A photo-electric device for the evaluation of structure factors. *Acta Crystallographica*, 2: 130-135.
- Luber, P., E. Bartelt, E. Genschow, J. Wagner and H. Hahn, 2003. Comparison of broth microdilution, E test and agar dilution methods for antibiotic susceptibility testing of *Campylobacter jejuni* and *Campylobacter coli*. *J. Clin. Microbiol.*, 41: 1062-1068.
- Mangalam, N.A., S. Sivakumar, S.R. Sheeja, M.R.P. Kurup and E.R.T. Tiekink, 2009. Chemistry of molecular and supramolecular structures of vanadium(IV) and dioxygen-bridged V(V) complexes incorporating tridentate hydrazone ligands. *Inorganica Chimica Acta.*, 362: 4191-4197.
- Mobinikhaledi, A., N. Forughifar and M. Kalhor, 2010. An efficient synthesis of Schiff bases containing benzimidazole moiety catalyzed by transition metal nitrates. *Turk. J. Chem.*, 34: 367-373.
- Moreno, E., S. Ancizu, S. Perez-Silanes, E. Torres, I. Aldana and A. Monge, 2010. Synthesis and antimycobacterial activity of new quinoxaline-2-carboxamide 1,4-di-N-oxide derivatives. *Eur. J. Med. Chem.*, 45: 4418-4426.
- Ogunniran, K.O., M.A. Mesubi, K.V.S.N. Raju and T. Narender, 2015. Structural and *in vitro* anti-tubercular activity study of (*E*)-*N'*-(2,6-dihydroxybenzylidene) nicotinohydrazone and some transition metal complexes. *J. Iran. Chem. Soc.*, 12: 815-829.
- Pavan, F.R., P.I.D.S. Maia, S.R.A. Leite, V.M. Deflon and A.A. Batista *et al.*, 2010. Thiosemicarbazones, semicarbazones, dithiocarbazates and hydrazide/hydrazones: Anti-*Mycobacterium tuberculosis* activity and cytotoxicity. *Eur. J. Med. Chem.*, 45: 1898-1905.
- Protopopova, M., C. Hanrahan, B. Nikonenko, R. Samala and P. Chen *et al.*, 2005. Identification of a new antitubercular drug candidate, SQ109, from a combinatorial library of 1,2-ethylenediamines. *J. Antimicrob. Chemother.*, 56: 968-974.
- Rakesh, D. Sun, R.B. Lee, R.P. Tangallapally and R.E. Lee, 2009. Synthesis, optimization and structure-activity relationships of 3,5-disubstituted isoxazolines as new anti-tuberculosis agents. *Eur. J. Med. Chem.*, 44: 460-672.
- Ramon-Garcia, S., R. Mikut, C. Ng, S. Ruden and R. Volkmer *et al.*, 2013. Targeting *Mycobacterium tuberculosis* and other microbial pathogens using improved synthetic antibacterial peptides. *J. Antimicrob. Agents Chemother.*, 57: 2295-2303.
- Ray, A., S. Banerjee, G.M. Rosair, V. Gramlich and S. Mitra, 2008. Variation in coordinative property of two different N_2O_2 donor Schiff base ligands with nickel(II) and cobalt(III) ions: Characterisation and single crystal structure elucidation. *Struct. Chem.*, 19: 459-465.
- Rollas, S. and S.G. Kucukguzel, 2007. Biological activities of hydrazone derivatives. *Molecules*, 12: 1910-1939.
- Sankar, R., S. Vijayalakshmi, S. Rajagopan and T. Kaliyappan, 2010. Synthesis, spectral, thermal and chelation potentials of polymeric hydrazone based on 2,4-dihydroxy benzophenone. *J. Applied Polym. Sci.*, 117: 2146-2152.
- Tachibana, M., M.M. Iwaizumi and S. Tero-Kubota, 1987. EPR studies of copper(II) and cobalt(II) complexes of adriamycin. *J. Inorgan. Biochem.*, 30: 133-140.
- Thomas, K.D., A.V. Adhikari, S. Telkar, I.H. Chowdhury and R. Mahmood *et al.*, 2011. Design, synthesis and docking studies of new quinoline-3-carbohydrazone derivatives as antitubercular agents. *Eur. J. Med. Chem.*, 46: 5283-5292.
- Torje, I.A., A.M. Valean and C. Cristea, 2012. Phenothiazine-carboxaldehyde-hydrazone derivatives synthesis, characterization and electronic properties. *Revue Roumaine Chimie*, 57: 337-344.
- Tripathi, L., R. Singh and J.P. Stables, 2011. Design and synthesis of *N'*-[substituted] pyridine-4-carbohydrazides as potential anticonvulsant agents. *Eur. J. Med. Chem.*, 46: 509-518.
- WHO., 2010. Global tuberculosis control report 2010. World Health Organization, Geneva, Switzerland. <http://afludiarly.blogspot.com/2010/11/who-global-tuberculosis-control-report.html>